Transmission by antiferromagnetic-nonmagnetic multilayers

1999 J. Phys.: Condens. Matter 11 2697

(http://iopscience.iop.org/0953-8984/11/13/007)

J. Phys.: Condens. Matter **11** (1999) 2697–2705. Printed in the UK PII: S0953-8984(99)97907-9

Transmission by antiferromagnetic–nonmagnetic multilayers

Jing-Ju Wang†, Xue-Fei Zhou†¶, Wei-Long Wan†[+], Xuan-Zhang Wang†‡ and D R Tilley§‖

† Department of Physics, Harbin Normal University, Harbin 150080, People's Republic of China
‡ CCAST (World Laboratory), PO Box 8730, Beijing 100080, People's Republic of China
§ School of Physics, Universiti Sains Malaysia, 11800USM Penang, Malaysia
‖ Department of Physics, University of Essex, Colchester CO4 3SQ, UK

Received 29 September 1998, in final form 23 December 1998

Abstract. The transmission of electromagnetic radiation at normal incidence through a finite antiferromagnetic–nonmagnetic superlattice is considered for an applied field normal to the interfaces (Faraday geometry) and for a field parallel to the interfaces (Voigt geometry). Besides the transmission spectra, we present the calculations of the dispersion curves for a relevant infinite superlattice to understand the features of the spectra. The transmission is weak or very weak at frequencies in the stop bands of the corresponding infinite superlattice, and these stop bands only appear at the Brillouin-zone edges $(2n + 1)\pi/D$, not at $2n\pi/D$.

1. Introduction

The long-wavelength dynamics of a magnetic material is governed by the frequency-dependent magnetic susceptibility tensor $\chi(\omega)$ which determines the magneto-optic properties. These may be seen by a gyromagnetic Fabry–Pérot resonator. For ferromagnets the interesting frequency range is microwave, but it is far infrared for antiferromagnets. If the magnetic film is not too thin exchange effects can be omitted and a complete account is given by a magnetic susceptibility tensor depending only on frequency. For this case, [1] has presented a comparatively complete theory and numerical calculations for the transmission of normally incident electromagnetic radiation through ferromagnetic and antiferromagnetic Fabry–Pérot resonators in both the Faraday (applied magnetic field perpendicular to plate) and Voigt (field parallel to plate) geometries. The results show that for unpolarized incident radiation, the Fabry–Pérot resonator can act as a tunable circular polarizer. When the film is very thin or the wave number $k \approx 1/D$ is large, then exchange effects should be included. The susceptibility tensor is a function of both frequency and wave number, that is, the system exhibits spatial dispersion. With the exchange interaction included [2], computed transmission spectra show that spin-wave fringes are unlikely to be observable for ferromagnets, but can be significant for thin antiferromagnetic films.

Recently we extended this kind of calculation to a Fabry–Pérot resonator in which the active material is a ferromagnetic–nonmagnetic superlattice [3, 4], where we present the explicit formulae for the bulk dispersion relation, and the transmission and reflection in

¶ Present address: Department of Physics, Heilongjiang College of Education, Harbin 150080, People's Republic of China.
[+] Present address: Department of Physics, Hulan Teacher's College, Hulan, Harbin 150000, People's Republic of China.

0953-8984/99/132697+09$19.50

normal incidence in the Faraday geometry (static field and ordering direction normal to the interface). The numerical calculations are given for the two optical eigenmodes which are the states of circular polarization. Electromagnetic propagation in a infinite superlattice is governed by the Bloch theorem so that stop bands appear at the Brillouin-zone edges. For a corresponding finite superlattice, the Bloch theorem, strictly speaking, is unavailable, but when the superlattice contains many unit cells, the transmission of electromagnetic radiation through it appears weak or may be very weak at frequencies in the stop bands of the relevant infinite superlattice. Consequently the transmission and reflection spectra become more complicated. In addition, although we omitted the effects of partial mirrors the fringes are still sharpened around resonance [3] as compared with [1], because the interfaces in the superlattice act as mirrors.

This paper extends the calculations in [3] and [4] to a Fabry–Pérot in which the active medium is an antiferromagnetic–nonmagnetic superlattice in the Faraday or Voigt geometry. The antiferromagnetic layers have uniaxial anisotropy and the nonmagnetic layers are an ordinary medium with magnetic permeability $\mu_n = 1.0$ and dielectric constant ε_n. Here we consider purely dipolarization effects and suppose that the power of the incident light is such that no nonlinear effects occur. In the Faraday geometry, the anisotropy axis and static magnetic field are taken perpendicular to the interfaces, and infrared electromagnetic radiation is incident normally on the superlattice, but in the Voigt geometry the axis and field are taken parallel to the interfaces and the incident radiation is still normal.

The finite superlattice, axes and notation to be applied are illustrated in figure 1 where electromagnetic radiation is incident normally on the upper surface of the superlattice and no matter which geometry we use, the anisotropy axis and static field are always parallel to the direction of magnetic ordering. The field, anisotropy axis and direction of magnetic ordering, however, are taken perpendicular to the interfaces in the Faraday geometry and parallel to the interfaces in the Voigt geometry. The superlattice is made up of thickness d_m of antiferromagnetic and d_n of nonmagnetic layers and contains N unit cells (or N bilayers). ε_m and $\boldsymbol{\mu}$ are the dielectric constant and magnetic permeability tensor of the antiferromagnetic layers and ε_n and $\mu_n(= 1.0)$ are the dielectric and permeability constants in the nonmagnetic layers. $D = d_m + d_n$ indicates the size of the unit cells and ε_1 and ε_2 refer to the upper and lower media.

For normally incident electromagnetic radiation, the electromagnetic field is proportional to $\exp(\pm \mathrm{i}k_m z - \mathrm{i}\omega t)$ in the magnetic layers, $\exp(\pm \mathrm{i}k_n z - \mathrm{i}\omega t)$ in the nonmagnetic layers, $\exp(\pm \mathrm{i}k_1 z - \mathrm{i}\omega t)$ in the medium above the superlattice and $\exp(+\mathrm{i}k_2 z - \mathrm{i}\omega t)$ in the medium below it, where + and − refer to waves propagating in the + and $-z$ directions. The wave numbers are given by a general formula

$$k^2 = \frac{\omega^2}{c^2}\varepsilon\mu \tag{1}$$

where ε is a dielectric constant and μ a magnetic permeability. μ is a constant for a nonmagnetic medium, but it is a function of frequency ω for the antiferromagnetic layers. In the Faraday geometry there are two eigenmodes corresponding to $\mu_+ = 1 + \chi_+$ and $\mu_- = 1 + \chi_-$, so that both k and μ in (1) carry the subscript + or −. For the Voigt geometry $\mu = [(2 + \chi_+ + \chi_-)^2 - (\chi_+ - \chi_-)^2]/[2(2 + \chi_+ + \chi_-)]$ which is the effective permeability μ_v. $\chi_\pm$ is [1]

$$\chi_\pm = \frac{-2\omega_m\omega_A(1+\eta^2) + \mathrm{i}(2\eta\omega\omega_m)}{\omega^2 \pm 2\omega\omega_0 + (\omega_0^2 - \omega_R^2)(1+\eta^2) + \mathrm{i}2\eta\omega(\omega_E + \omega_A)} \tag{2}$$

where η represents the Landau–Lifshitz damping and ω_0, ω_A and ω_E are related to the static magnetic, anisotropy and exchange field by $\omega_0 = \gamma H_0$, $\omega_A = \gamma H_A$ and $\omega_E = \gamma H_E$.

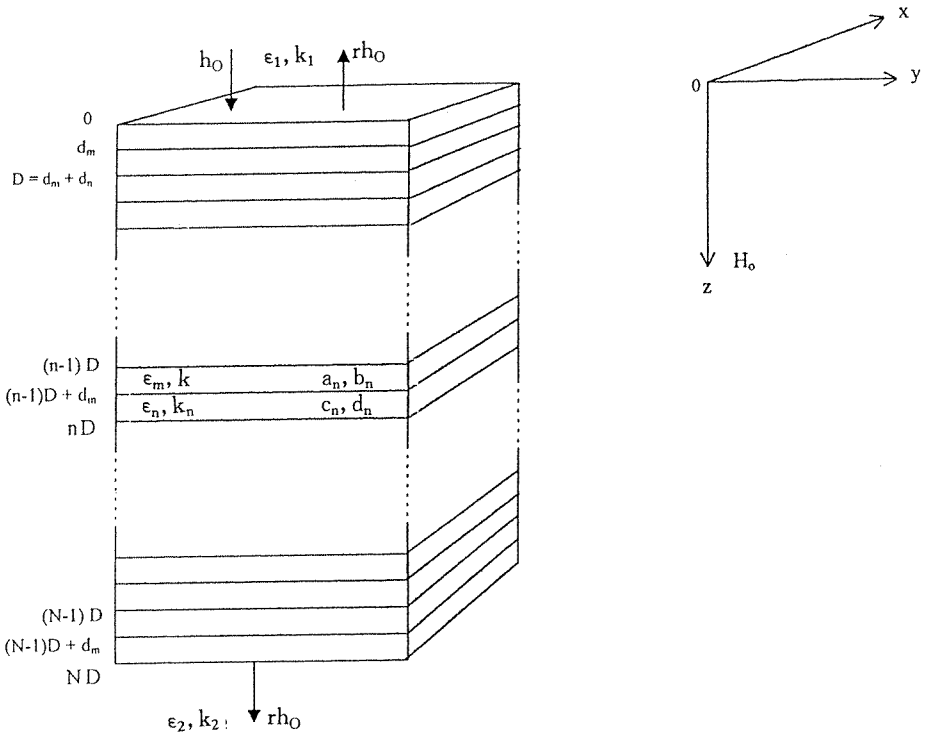

Figure 1. Finite antiferromagnetic–nonmagnetic superlattice with axes and notation used in the paper. Description in detail is presented in the text.

$\omega_R = \sqrt{2\omega_A\omega_E + \omega_A^2}$ is the antiferromagnetic resonance frequency and γ is the gyromagnetic ratio. In contrast to [2], here the exchange term (Dk^2) is omitted.

The calculations and discussion for the dispersion relation is presented in the second section, where we give the dispersion relation of the relevant infinite superlattice (k as a function of ω). In section 3, we first recall briefly the main theoretical results for the transmission and then the numerical results and discussion are presented. Finally we put the conclusion in section 4.

2. Dispersion relation

As the previous section describes, the optical properties of an infinite superlattice are governed by the Bloch theorem, but for multilayers of finite thickness this theorem, strictly speaking, does not apply. However, if the finite system contains many unit cells, phenomena similar to those resulting from the theorem, may appear in different degrees and some of these phenomena are seen from the transmission spectra of electromagnetic radiation. Thus we first discuss the dispersion relation of an infinitely extended antiferromagnetic–nonmagnetic superlattice together with numerical results.

According to the transformation matrix method [4, 6] (see the appendix) for electromagnetic radiation propagating normal to the interfaces of the superlattice

$$\begin{pmatrix} a_{n+1}^U \\ b_{n+1}^U \end{pmatrix} = \overleftrightarrow{T} \begin{pmatrix} a_n^U \\ b_n^U \end{pmatrix} \tag{3}$$

where a_n^u and b_n^u represent the amplitudes of waves at the upper surface of the nth antiferromagnetic layer. $\overleftrightarrow{T}$ is the transformation matrix

$$\overleftrightarrow{T} = \begin{pmatrix} A & B \\ B^* & A^* \end{pmatrix} \tag{4}$$

B^* and A^* are the complex conjugates of B and A, which are determined as

$$A = \delta \left[\frac{\mathrm{i}(1+\Delta^2)}{2\Delta} \sin k_n d_n + \cos k_n d_n \right] \tag{5}$$

and

$$B = \delta^{-1} \left[\frac{1(1-\Delta^2)}{2\Delta} \sin k_n d_n \right] \tag{6}$$

by using the general electromagnetic boundary conditions between two different layers. In (5) and (6) $\delta = \exp(\mathrm{i}k_m d_m)$ and $\Delta = \varepsilon_n k_m / \varepsilon_m k_n$, and the subscripts m and n indicate the antiferromagnetic and nonmagnetic layers respectively. The dispersion relation is given by

$$\cos(QD) = \mathrm{Tr}(\overleftrightarrow{T})/2 = (A + A^*)/2 \tag{7}$$

with Q the Bloch wave vector. Equations (5) to (7) are the main theoretical results in this section. In order to see clearly the physics included in this equation, we now present numerical calculations. The parameters are taken as follows: $\varepsilon_m = 5.5$, $H_A = 19.7$ T, $H_E = 53.3$ T, $M_s = 0.056$ T and $\gamma = 1.05$ (cm^{-1} T^{-1}) corresponding to FeF_2; $\varepsilon_n = 5.5$, $H_0 = 3.15\ M_s$ or $H_0 = 0.0$. For an antiferromagnet, like FeF_2 or MnF_2, with a perfect crystal structure at low temperature, the damping is very weak so that it is often omitted when one calculates the dispersion relation, but for the calculations of transmission, reflection spectra or the ATR spectra, one has to add the damping's effects in the calculations [5]. Recently, there have been some works [8, 9] dealing with the effects of the damping on the dispersion properties of metal magnetic systems, where the damping is larger. In this section, we omit the damping for calculations of the dispersion relation.

Figure 2 illustrate the dispersion properties of the infinite superlattice in a static magnetic field normal to the interfaces (Faraday geometry) and figure 3 shows those of the superlattice in a static magnetic field parallel to the interfaces (Voigt geometry). We should note that the magnetic anisotropy axis is parallel to the field in each geometry, so the anisotropy axes in the two geometries are different. When $H_0 = 0$ the dispersion figures for the two states of circular polarization in the Faraday geometry are the same (see figure 2(a)). The dispersion curve shows a very narrow stop band at the resonance frequency $\omega_R = 52.45$ cm^{-1} together with stop bands at the zone faces. The superlattice period D is smaller by a factor of 10 in figure 2(b) compared with figure 2(a) and the frequency scale is correspondingly expanded by a factor of 10. In contrast to the ferromagnetic/nonmagnetic superlattice [3], the stop bands only appear at $(2n+1)\pi/D$ while there are no stop bands at $2n\pi/D$ where $n = 0, 1, 2, 3, \ldots$. This property is distinctive. In a non-zero field H_0 in the Faraday geometry the usual Zeeman splitting [5] appears between the two circular-polarization states but there are no other significant changes so the dispersion curves are not shown.

In the Voigt geometry the propagating eigenmodes are the plane-polarization states, the state with h field transverse to H_0 being coupled to the magnetic resonances and the state with h along H_0 uncoupled [1]. The dispersion curves shown are for the former. There is a double resonance near ω_R due to the Voigt permeability μ_V and otherwise stop bands are seen at the zone edges. As in figures 2(a) and 2(b), non-zero stop bands occur only at odd-integer multiples of QD/π and as in those figures, the difference in frequency scale between figures 3(a) and 3(b) is due to a factor of ten difference in D. For a finite magnetic superlattice,

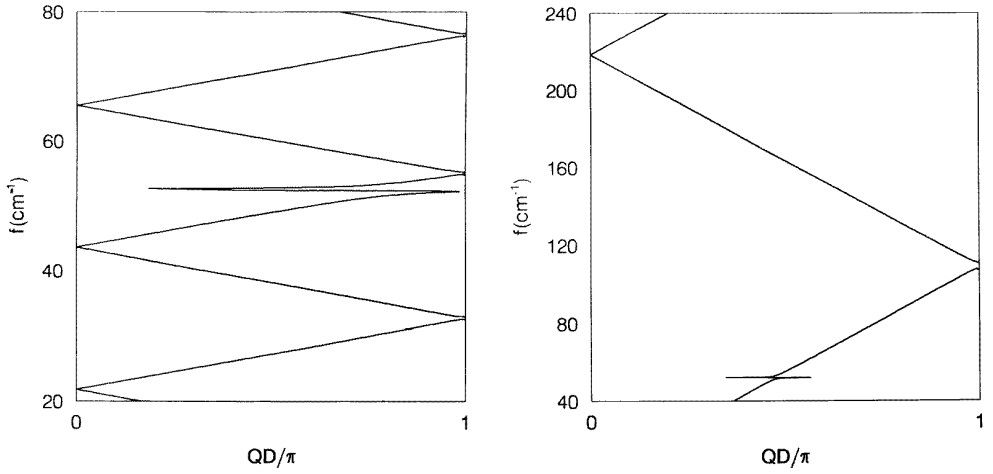

(a) (b)

Figure 2. Dispersion curves of the infinite superlattice in the Faraday geometry: (a) $d_m = d_n = 0.01$ cm and $H_0 = 0.0$, (b) $d_m = d_n = 0.001$ cm and $H_0 = 3.15\ M_s$ for the + state of circular polarization.

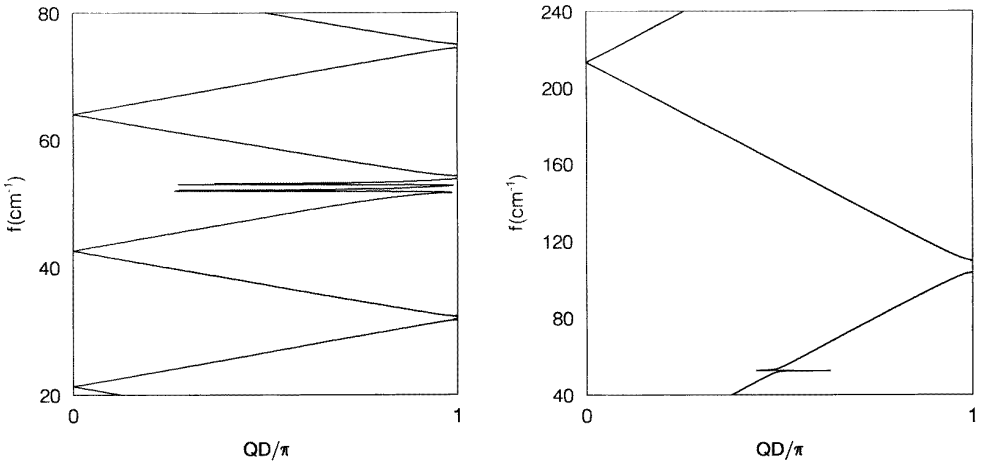

(a) (b)

Figure 3. Dispersion curves of the infinite superlattice in the Voigt geometry: (a) $d_m = d_n = 0.01$ cm and $H_0 = 3.15\ M_s$, (b) $d_m = d_n = 0.001$ cm and $H_0 = 3.15\ M_s$.

the Bloch theorem, strictly speaking, is unavailable, but the transmission of electromagnetic radiation through the superlattice is weak, maybe very weak, at frequencies in the stop bands of the relevant infinite superlattice. This point can be seen from the figures in the next section.

3. Transmission spectra

We assume that the finite superlattice contains N unit cells (thickness ND) with medium 1 above and medium 2 below. Incident and reflected electromagnetic radiation are in medium 1 and transmitted radiation in medium 2. According to the transformation matrix method (see the

appendix for the main points), the relation between coefficients (a_1^u, b_1^u) in the first magnetic layer and (a_N^u, b_N^u) in the Nth magnetic layer is

$$\begin{pmatrix} a_N^u \\ b_N^u \end{pmatrix} = \overleftrightarrow{T}^{N-1} \begin{pmatrix} a_1^u \\ b_1^u \end{pmatrix} = \begin{pmatrix} D_{11} & D_{12} \\ D_{21} & D_{22} \end{pmatrix} \begin{pmatrix} a_1^u \\ b_1^u \end{pmatrix} \tag{8}$$

with $\overleftrightarrow{T}$ given by (4), D_{ij} being the elements of $\overleftrightarrow{T}^{N-1}$. When using the boundary conditions to derive the expression of transmission coefficient t, we should note that the last layer is a nonmagnetic layer. Thus we obtain the transmission amplitude

$$t = [4\Delta\Delta_2(D_{12}D_{21} - D_{11}D_{22})]/[\delta(g - \Delta_2 h)[(D_{11} - D_{12}) - \Delta_1(D_{11} + D_{12})] + \delta^{-1}(g^* + \Delta_2 h^*)[(D_{21} - D_{22}) - \Delta_1(D_{21} + D_{22})]]^{-1} \tag{9}$$

where $\Delta_1 = \varepsilon_1 k_m/\varepsilon_m k_1$, $\Delta_2 = \varepsilon_2 k_n/\varepsilon_n k_2$,

$$g = \cos k_n d_n + \mathrm{i}\Delta \sin k_n d_n \tag{10a}$$

and

$$h = \Delta \cos k_n d_n + \mathrm{i} \sin k_n d_n. \tag{10b}$$

As before, $\delta = \exp(\mathrm{i}k_m d_m)$ and $\Delta = \varepsilon_n k_m/\varepsilon_m k_n$.

In numerical calculations, we take $\varepsilon_1 = \varepsilon_2 = 1.0$ and the other parameters have been given the last section. For calculations of the transmission coefficient, one should consider the effects of damping η in (2) and we let the damping factor $\eta = 0.0001$.

We find in the Faraday geometry that, except that the + and − states of electromagnetic radiation have different resonant frequencies in a static magnetic field, their transmission patterns are basically the same. Thus we only present the figures for the + state in figure 4 where the transmission is described by $T = |t|^2$. For $d_m = d_n = 0.01$ cm and $N = 10$, figure 4(a) shows a narrow transmission zero at the resonance frequency and also transmission anomalies at the positions of the stop bands related to the Brillouin-zone edges $(2n+1)\pi/D$ in figure 2(a). No anomalies appear for Q near to 0 because the system with ten superlattice cells is much more different from a infinite superlattice. For $d_m = d_n = 0.001$ cm and $N = 100$,

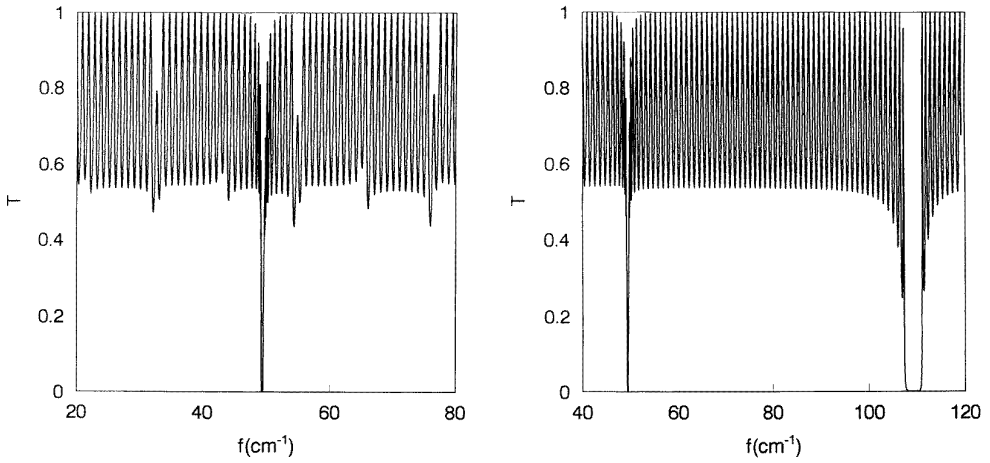

Figure 4. Calculated transmission curves for the Faraday geometry: (*a*) $d_m = d_n = 0.01$ cm, $H_0 = 3.15\ M_s$ and $N = 10$ for the + state of circular polarization; (*b*) $d_m = d_n = 0.001$ cm, $H_0 = 3.15\ M_s$ and $N = 100$ also for the + state.

from figure 4(b) one can see the resonance zero and a well developed zero at $f = 110$ cm^{-1} corresponding to the stop band in figure 2(b). Fringes resulting from the overall thickness ND are seen elsewhere.

The Voigt-geometry transmission graphs for the plane polarization that couples to the magnetic properties are shown in figures 5(a) and 5(b), which correspond to the dispersion curves of figures 3(a) and 3(b). The former shows narrow transmission zeros at about 50 and 56 cm^{-1} resulting from the two resonance frequencies and also low-transmission intervals arising corresponding to the stop bands at 32, 54 and 74 cm^{-1} in figure 3(a). In figure 5(b) the resonance zeros are still seen and, in addition, the quasi-stop band from 105 to 110 cm^{-1} is very well developed because of the larger value of N. The reason is that for a larger value of N, the superlattice is more similar to the relevant infinite superlattice so that the transmission is more difficult.

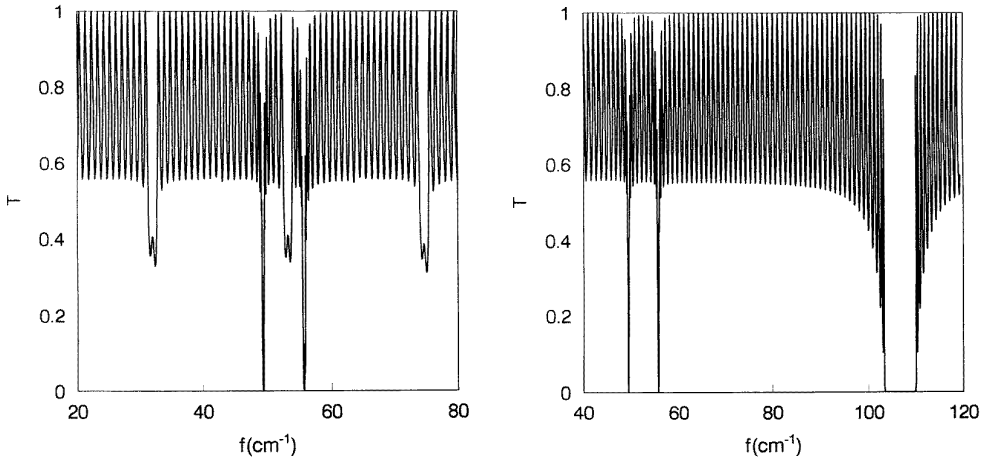

Figure 5. Calculated transmission curves for the Voigt geometry: (*a*) $d_m = d_n = 0.01$ cm, $H_0 = 3.15\ M_s$ and $N = 10$; (*b*) $d_m = d_n = 0.001$ cm, $H_0 = 3.15\ M_s$ and $N = 100$.

4. Conclusion

We have investigated the transmission spectra of the finite antiferromagnetic–nonmagnetic superlattice in both the Faraday geometry and Voigt geometry and, in order to understand their features, presented the numerical calculations of the dispersion relation for the relevant infinite superlattice. The parameters selected for numerical calculations are those of FeF_2/ZnF_2 superlattices. Generally speaking, the range of interesting frequency for antiferromagnets is the far infrared so that frequency scanning is practical for transmission spectra [5]. Our system can be considered as a Fabry–Pérot etalon, without the mirrors, made of a finite antiferromagnetic–nonmagnetic superlattice so that the properties described in the paper can be studied experimentally, as in [7] where Sanders *et al* measured transmission of FIR radiation through discs of FeF_2.

It is interesting that the stop bands only exist at the Brillouin-zone edges $(2n+1)\pi/D$, but do not appear at $2n\pi/D$ (where $n = 0, 1, 2, 3, \ldots$) for the infinite antiferromagnetic–nonmagnetic superlattice. For a fixed thickness of the finite superlattice, the more unit cells are contained in the superlattice, the weaker the transmission, at frequencies in the stop bands of the infinite

superlattice, is. In addition, the stop bands are wider and clear in the Voigt geometry than in the Faraday geometry.

Strictly speaking, the Bloch theorem is unavailable for a finite superlattice, but the transmission of electromagnetic radiation through the finite superlattice must be difficult at frequencies in the stop bands of the relevant infinite superlattice. For a superlattice with a very large value of N, the quasi-stop bands can be seen clearly from the transmission spectra or reflection spectra.

Acknowledgments

This work was supported by the National Natural Science Foundation of China through grant 19574014, by the Outstanding Youth Science Foundation of Heilongjiang Province and by the Malaysian Government IRPA grant 09-02-05-6001. XZW also acknowledges the Third World Academy of Science and Universiti Sains Malaysia for support to visit USM.

Appendix

In this appendix, we present the main points of the transfer matrix method in the text. According to figure 1, we write the electromagnetic h fields in terms of the incident amplitude h_0 as

$$h = h_0 \exp(\mathrm{i}k_1 z) + r h_0 \exp(-\mathrm{i}k_1 z) \qquad \text{upper medium} \tag{A1}$$

$$\begin{aligned} h &= a^u_{n+1} h_0 \exp[\mathrm{i}k_m(z - nD)] + b^u_{n+1} h_0 \exp[-\mathrm{i}k_m(z - nD)] \\ &= a^b_{n+1} h_0 \exp[\mathrm{i}k_m(z - nD - d_m)] + b^b_{n+1} h_0 \exp[-\mathrm{i}k_m(z - nD - d_m)] \\ &\qquad \text{antiferromagnetic layer } n+1 \end{aligned} \tag{A2}$$

$$\begin{aligned} h &= c^u_{n+1} h_0 \exp[\mathrm{i}k_n(z - nD - d_m)] + d^u_{n+1} h_0 \exp[-\mathrm{i}k_n(z - nD - d_m)] \\ &= c^b_{n+1} h_0 \exp\{\mathrm{i}k_n[z - (n+1)D]\} + d^b_{n+1} h_0 \exp\{-\mathrm{i}k_n[z - (n+1)D]\} \\ &\qquad \text{nonmagnetic layer } n+1 \end{aligned} \tag{A3}$$

$$h = t h_0 \exp[\mathrm{i}k_2(z - nD)] \qquad \text{lower medium.} \tag{A4}$$

It simplifies the formalism to use amplitudes $(a^{u,b}_n, b^{u,b}_n)$ and $(c^{u,b}_n, d^{u,b}_n)$ containing a phase factor relating to a local z origin at the top (u) and bottom (b) of the layer; equivalent amplitudes are related by simple phase matrices:

$$\begin{pmatrix} a^b_n \\ b^b_n \end{pmatrix} = \begin{pmatrix} \delta & 0 \\ 0 & \delta^{-1} \end{pmatrix} \begin{pmatrix} a^u_n \\ b^u_n \end{pmatrix} \tag{A5}$$

and

$$\begin{pmatrix} c^b_n \\ d^b_n \end{pmatrix} = \begin{pmatrix} \delta_n & 0 \\ 0 & \delta_n^{-1} \end{pmatrix} \begin{pmatrix} c^u_n \\ d^u_n \end{pmatrix} \tag{A6}$$

where $\delta_n = \exp(\mathrm{i}k_n d_n)$ and δ is given in the text. The complex amplitudes in the different layers are related by the electromagnetic boundary conditions at the interfaces. Within the superlattice these give

$$a^b_n + b^b_n = c^u_n + d^u_n \tag{A7}$$

$$\Delta(a^b_n - b^b_n) = c^u_n - d^u_n \tag{A8}$$

$$a^u_{n+1} + b^u_{n+1} = c^b_n + d^b_n \tag{A9}$$

$$\Delta(a^u_{n+1} - b^u_{n+1}) = c^b_n - d^b_n \tag{A10}$$

with Δ defined in the text. Combining (A5) to (A10) we find the transfer matrix for propagation across a unit cell of the superlattice, or

$$\overleftrightarrow{T} = \begin{pmatrix} A & B \\ B^* & A^* \end{pmatrix} \tag{A11}$$

and

$$\begin{pmatrix} a^u_{n+1} \\ b^u_{n+1} \end{pmatrix} = \overleftrightarrow{T} \begin{pmatrix} a^u_n \\ b^u_n \end{pmatrix} \tag{A12}$$

with A and B given by (5) and (6) in the text. The dispersion relation of the infinite superlattice, then, is

$$\cos(QD) = \tfrac{1}{2}\mathrm{Tr}(\overleftrightarrow{T}) \tag{A13}$$

where Q is the Bloch wave vector. For transmission across the whole superlattice we have

$$\begin{pmatrix} a^u_n \\ b^u_n \end{pmatrix} = \overleftrightarrow{T}^{N-1} \begin{pmatrix} a^u_1 \\ b^u_1 \end{pmatrix} = \begin{pmatrix} D_{11} & D_{12} \\ D_{21} & D_{22} \end{pmatrix} \begin{pmatrix} a^u_1 \\ b^u_1 \end{pmatrix}. \tag{A14}$$

These are the main idea and formulae of the transfer matrix method. Using these formulae, we can obtain the main theoretical results in the text.

References

[1] Lim Siew-Choo, Osman J and Tilley D R 1997 *J. Phys.: Condens. Matter* **9** 8297

[2] Lim Siew-Choo, Osman J and Tilley D R 1998 *J. Phys.: Condens. Matter* **10** 1891

[3] Zhou X F, Wang J J, Wang X Z, Lim S C, Osman J and Tilley D R 1998 *Conf. Digest, 23rd Int. Conf. on Infrared and Millimeter Waves (University of Essex, UK, 7–11 September 1998)* ed T J Parker and S R P Smith

[4] Zhou Xue-Fei, Wang Jing-Ju, Wang Xuan-Zhang and Tilley D R unpublished

[5] Abraha K and Tilley D R 1996 *Surf. Sci. Rep.* **24** 125

[6] Raj N and Tilley D R 1989 *The Dielectric Function of Condensed Systems* ed L V Keldysh, D A Kirzhnitz and A A Maradudin (Amsterdam: Elsevier) ch 7

[7] Sanders R W, Belanger R M, Motokawa M, Jaccarino V and Rezende S M 1981 *Phys. Rev.* B **23** 1190

[8] Almeida N S and Mills D L 1996 *Phys. Rev.* B **53** 12 232

[9] Jia Cheng, Wang Xuan-Zhang and Lu Shu-Chen 1999 *Phys. Rev.* B **59** 3310